

Monte Carlo study of linear chain submonolayer structures. Application to Li/W(112)

Czesław Oleksy

Institute of Theoretical Physics, University of Wrocław

Plac Maksa Borna 9, 50-204 Wrocław, Poland

(Dated: November 15, 2018)

The lattice gas model for adsorption of alkaline elements on W(112) surface is studied by Monte Carlo simulations. The model includes dipole–dipole interaction as well as long-range indirect interaction. The numerical results show that truncation of the indirect interaction even at 200\AA may change a phase diagram, i.e., new phases containing domain walls might occur. It is demonstrated that a defected phase can exist at high temperatures even if it is not stable at $T=0$. The phase diagram for Li/W(112) is constructed and long periodic chain structures (9×1) , (6×1) , (4×1) , (3×1) , and (2×1) are found to be stable at low temperatures. Role of thermal fluctuation is discussed by comparison of Monte Carlo results with mean field approximation results.

PACS numbers: 68.35.Rh, 05.10.Ln

I. INTRODUCTION

Chemisorption on metal surfaces has been studied for over 30 years^{1,2,3,4,5,6,7,8,9}. One of interesting problems concerns with structures and phase transitions in chemisorbed submonolayers. In particular alkaline, alkaline–earth, and rare-earth elements adsorbed on W(112) and Mo(112) form linear chain structures^{1,7}. In case of low coverages ($\Theta < 0.5$), the commensurate phases with chains normal to the troughs of the substrate are observed. The period of these structures changes from 2 to 9^1 . At higher coverages ($\Theta > 0.5$), incommensurate surface phases occur^{8,9}. It has been suggested^{1,4} that formation of chain structures might be due to indirect interaction between adatoms via conduction electrons. Recently we proposed¹⁰ the lattice gas model to account for linear chain structures on W(112) and Mo(112). The model includes dipole–dipole interaction as well as indirect oscillatory interaction. As the interactions are of long range, the model is difficult to study theoretically. Preliminary studies performed in molecular field approximation confirmed that competition of dipole-dipole interaction and indirect interaction leads to formation of linear chain structures. Further extensive analysis of ground states in related effective one-dimensional model with infinite range of interactions¹¹ pointed out that competition between these two interactions is crucial in formation of linear chain structures. In very recent investigation of phase transitions in Li/Mo(112) and Sr/Mo(112), H. Pfnür et al.^{7,12,13} have shown that the lattice gas model could be useful in description of long periodic phases observed at low coverages. Results of their investigation support an idea that surface electronic state are responsible for the oscillatory indirect interaction between adatoms.

It is intention of this paper to study phase diagrams by Monte Carlo simulations. This method was successfully applied to lattice gas models with short range interactions^{14,15,16,17}. On the other hand, one can expect

more difficult problems in case of long range interactions, e.g., occurrence of complicated structures^{18,19,20,21}. The paper is organized as follows. In section 2 the lattice gas model is described. Two difficulties connected with application of Monte Carlo simulations to this model are discussed in section 3. In section 4 phase diagrams are presented and section 5 contains discussion and conclusions.

II. THE MODEL

In the previous paper¹⁰ we introduced the lattice gas model of linear chain submonolayer structures on the (112) surface of W and Mo. Adsorption sites form the rectangular lattice (see Fig. 1) with $a_x = a\sqrt{2}$ and $a_y = a\sqrt{3}/2$, where a denotes the lattice constant of the bcc elementary cell. The model Hamiltonian within the grand canonical ensemble, is defined as

$$\mathcal{H} = \frac{1}{2} \sum_{\substack{i,j \\ j \neq i}} V_{ij} n_i n_j - \mu \sum_i n_i \quad , \quad (1)$$

where n_i is the occupation variable at each adsorption site i with $n_i = 1$ if the i th site is occupied by an adatom and $n_i = 0$, if not. The chemical potential is denoted by μ and $V_{ij} = V(\vec{r}_i - \vec{r}_j)$ is the pairwise interaction consisting of electrostatic and indirect interactions

$$V(\vec{r}) = \frac{2d^2}{|\vec{r}|^3} + \begin{cases} A \cos(2k_F|y| + \varphi) \frac{1}{|y|} \delta(x, 0) & \text{for } y \neq 0 \\ E_b \delta(|x|, a_x) & \text{for } y = 0 \end{cases} \quad (2)$$

The first part of Eq. (2), $2d^2/|\vec{r}|^3$, describes a repulsive dipole-dipole interaction between two adatoms with identical dipole moments d . The second term in Eq. (2) represents an asymptotic part of the indirect interaction between adatoms via conduction electrons of the substrate. This particular interaction is highly anisotropic

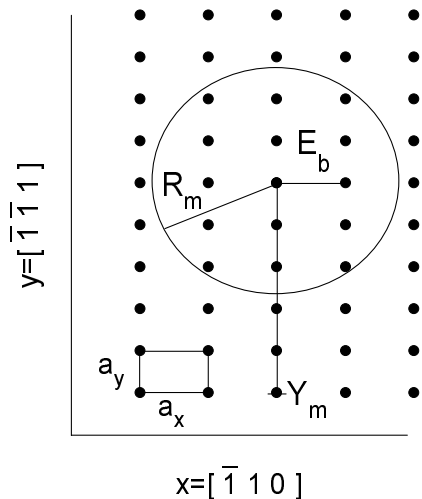


FIG. 1: A lattice of adsorption sites on (112) surface of *bcc* metal. The elementary cell is drawn in the left corner. Ranges of two-particles interactions used in simulations are depicted. For a notation see the text.

and is closely related to the existence of nearly flattened segments of the Fermi surface being perpendicular to the $[\bar{1}\bar{1}1]$ axis directed along the atomic troughs of the substrate^{4,10}. It is also possible that contribution to this interaction comes from quasi-one-dimensional surfaces states²². Very recently, G. Godzik et al.¹³ suggested that oscillatory indirect interaction of this form is, in case of Sr/Mo(112), induced by charge density waves involving surfaces states. An amplitude A and a phase φ can be treated as phenomenological parameters and k_F denotes a wavevector of electrons at the Fermi surface. Finally, for $y = 0$ there is an attractive indirect interaction E_b between the nearest neighbours along the x -direction which is responsible for the chain formation.

In this work we choose the set of model parameters the same as proposed in the previous paper¹⁰ for adsorption of lithium on W(112) surface, i.e., $d = 1.5D$, $A = -0.137eV\text{\AA}$, $k_F = 0.41\text{\AA}^{-1}$, $\varphi = 1.26\pi$, $E_b = -0.05eV$, and $a = 3.16\text{\AA}$. We will use a reduced chemical potential μ/μ_0 with $\mu_0 = k_B T$, $T = 100K$. Although the interaction described by Eq. (2) is long-range we introduce finite range of this interaction in Monte Carlo study. The dipole-dipole interaction is accounted for distances between adatoms smaller than R_m and the indirect interaction along the y -direction for distances smaller than Y_m (see Fig. 1).

The adatom coverage θ is defined as

$$\theta = \frac{1}{N} \sum_i \langle n_i \rangle, \quad (3)$$

where N is the number of adsorption sites and angle brackets mean a thermodynamic average.

It is convenient to transcript the lattice gas model as

Ising model by introducing spin variables $s_i = 1 - 2n_i$

$$\mathcal{H} = \frac{1}{8} \sum_{\substack{i,j \\ j \neq i}} V_{ij} s_i s_j - H \sum_i s_i, \quad (4)$$

where the magnetic field H is expressed by the chemical and interaction potentials:

$$H = -\frac{\mu}{2} + \frac{1}{4} \sum_j V_{ij}. \quad (5)$$

Using Ising Hamiltonian, Eq. (4), we can perform simulation in the canonical ensemble which is equivalent to simulation of the lattice gas, Eq. (1), in the grand canonical ensemble. Of course, the former method is much easier.

III. MONTE CARLO METHOD

In Monte Carlo simulation we employ standard Metropolis algorithm to Ising Hamiltonian, Eq. (4), on finite rectangular lattice of $L_x \times L_y$ sites with periodic boundary conditions (PBC). Quantities such as magnetisation M , specific heat C_H , and energy E are obtained as

$$M = \frac{1}{N} \sum_i \langle s_i \rangle, \quad (6)$$

$$C_H = \frac{1}{Nk_B T^2} (\langle \mathcal{H}^2 \rangle - \langle \mathcal{H} \rangle^2), \quad (7)$$

$$E = \frac{1}{N} \langle \mathcal{H} \rangle, \quad (8)$$

where $N = L_x L_y$ is the number of spins. We will use the relation between coverage θ and the magnetisation M : $\theta = (1 - M)/2$. Since we are interested in linear chain structures we measure also magnetisation at each row of the lattice

$$M_j = \frac{1}{L_x} \sum_i \langle s_{\mathbf{r}_i^{(j)}} \rangle, \quad (9)$$

where

$$\mathbf{r}_i^{(j)} = (ia_x, ja_y),$$

Having M_j one can calculate coverage at j th lattice row $\theta_j = (1 - M_j)/2$.

To study phase diagram we calculate the correlation function $\langle s_j s_l \rangle$ and the structure factor defined as¹⁴

$$S(q) = \frac{1}{N^2} \sum_{j,l} \langle s_j s_l \rangle \exp(i\mathbf{q}(\mathbf{r}_j - \mathbf{r}_l)), \quad (10)$$

where q is a wavevector from reciprocal space. This function is used to recognize an ordered phase.

We encountered two difficulties in examination of phase diagrams by Monte Carlo method:

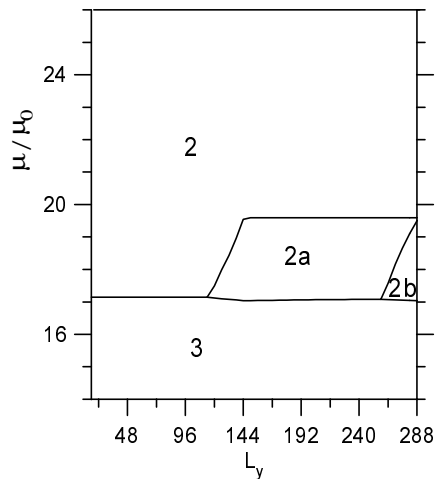


FIG. 2: Ground states in the chemical potential / lattice size L_y plane for range of indirect interaction $Y_m = 72$. Regions denoted by 2 and 3 correspond to phases (2×1) and (3×1) . For detailed description of states $2a$ and $2b$ see the text.

- (1) The dependence of the results on range of the indirect interaction.
- (2) The dependence of the resulting spin structure, at low temperatures, on an initial spin configuration.

In the previous paper¹⁰ we studied this model within the molecular field approximation (MFA) finding several ordered phases of $(p \times 1)$ type in phase diagrams. The $(p \times 1)$ structure at $T = 0$, has every jp row (for $j = 1, 2, \dots, L_y/p$) occupied by adatoms and remaining rows are empty. Therefore, coverage in this structure $\theta = 1/p$ and the structure factor $S(q)$ reaches maximum at $q = (0, 2\pi/(pa_y))$. The phase diagram constructed for the Li/W(112) system contains the (2×1) , (3×1) , (4×1) , (6×1) , and (9×1) linear chain structures. Performing Monte Carlo simulations we observed that additional ordered structures can occur in a phase diagram. It may happen when the range of indirect interaction Y_m is shorter than the linear lattice size along the y-direction L_y . We start investigation of this problem by checking the influence of indirect interaction range on the ground states. As an example we present in Fig. 2 a part of ground-state diagram for constant range of interaction $Y_m = 72$ and different values of the lattice size L_y . We see that only two phases, (2×1) and (3×1) , are present in this part of phase diagram when the interaction range Y_m is close to the lattice size ($L_y < 108$). An additional phase denoted as $(2a)$ appears for $L_y > 108$. This is linear chain structure consisting of two domains of the (2×1) phase and separated by two empty rows. Thus it has coverage $\theta = (L_y - 2)/(2L_y)$. It is worth noting that the (2×1) phase has two domains: one with adsorbate chains placed in even lattice rows and the second with chains in odd rows. The configuration of the $(2a)$ phase at $L_y = 144$ may be represented by

sequence of distances between subsequent chains in the following way $\{2_{35}, 3_1, 2_{34}, 3_1\}$, where l_j denotes sequence of j identical distances l . When range of interaction is nearly $1/4$ of L_y then another phase $(2b)$, containing four domain walls, occurs in the phase diagram (see Fig. 2). It looks like double $(2a)$ phase, e.g., the $(2b)$ phase can be represented by following sequences of distances $\{2_{34}, 3_1, 2_{34}, 3_1, 2_{31}, 3_1, 2_{27}, 3_1\}$ for $L_y = 264$. In a part of diagram corresponding to lower coverage (not shown in Fig. 2) there are also phases containing walls and domains of (4×1) , and (6×1) long periodic structures but detailed discussion will not be presented here. It worth to mention at this place, that the $(2a)$ phase can occur in the temperature phase diagram, even if the $(2a)$ phase is not a ground state. In order to check the role of the boundary conditions, we performed additional calculation of the ground states using free edge boundary condition along the y-direction. The same defected phases were obtained but the number of domain walls was reduced by one. Above discussion shows that truncation of long-range indirect interaction in our model causes some technical difficulties in applying Monte Carlo method, e.g. it can be impossible to study finite-size scaling. On the other hand, the truncation of the interaction interpreted as screening effect might be important from physical point of view because it generates defected phases containing domain walls.

The second problem observed in our Monte Carlo calculation, dependence of resulting configuration on the initial spin configuration, is due to presence of short range attractive interaction between the nearest neighbours along the x-direction. When linear chain structure is formed at low temperature, it is difficult to change the period of such structure by changing temperature or chemical potential using single spin flip Metropolis algorithm. We study a phase diagram performing MC runs at constant magnetic field (or chemical potential) by cooling down or heating up the sample. The simulation start from high temperature in the cooling down process and after thermalization and measurement temperature is lowering the by ΔT then such procedure is repeated till $T = 0$. At each temperature, all quantities are measured after 2×10^4 MC steps per spin during subsequent 5000 MC steps. The final spin configuration at T is used as initial one at $T - \Delta T$. For some values of H the cooling down process finishes at $T = 0$ with configuration having energy greater than energy of ground-state. Hence this way can produce metastable phases. To overcome this problem we use heating up process which starts at temperature ΔT with ground-state configuration as the initial spin configuration. In subsequent temperature steps, $T_i = T_{i-1} + \Delta T$, the specific heat C_H and the mean energy $\langle \mathcal{H} \rangle$ are measured. This allow us to calculate the entropy

$$S(T) = \int_0^T \frac{C_H(T')}{T'} dT',$$

by numerical integration. Then the free energy can be

obtained as

$$F(T) = \langle \mathcal{H} \rangle - TS(T).$$

Repeating simulations at given H with different ground-state configurations as initial configurations, we can find a phase with the lowest free energy at temperature T .

IV. PHASE DIAGRAMS

To study phase diagrams by Monte Carlo simulations we used method described in the previous section, i.e., simulations at constant chemical potential (or magnetic field) with variable temperature. The phase transition between ordered phases is determined by examination of free energies of appropriate phases. Temperature of transition from disordered phase to an ordered one is determined from behaviour of the structure factor $S(q)$, specific heat C_H or sublattice magnetisation M_j . Lattice sizes L_x, L_y used in our simulations are rather small due to long-range interaction and large number of MC runs needed to construct phase diagrams. Most simulations were performed for 20×72 lattice sites, but some calculations were performed on 40×72 and 20×144 . Periodic boundary conditions were assumed, therefore L_y was chosen as multiplicity of 36 in order to allow formation of ideal chain structures with period 2, 3, 4, 6, and 9, which exist in the ground-state phase diagram.

It has been shown in the previous section that defected ordered structure can occur when $Y_m < L_y$. We now discuss the thermal stability of such structure for two sets of parameters L_y and Y_m . We see in Fig. 3a that the (2a) phase dominates the part of phase diagram corresponding to intermediate coverage and it pushes down the phase (2×1) . Hence, it is impossible to pass directly from the ordered (2×1) phase to the disordered phase. More interesting case is shown in Fig. 3b where the (2a) phase occurs at high temperatures, although it is not stable at $T=0$. In this case, the (2a) phase is also placed between the (2×1) phase and the disordered phase. We think, that this is important result because it shows that analysis of the ground states is not sufficient to find all ordered phases. The phase (2a) has two interesting features

- (1) The wavevector $q = (0, 2\pi(L_y - 2)/(2L_y a_y))$, at which the structure factor has maximum, does not depend on temperature.
- (2) The sublattice order parameters vanish at some temperatures whereas the behaviour of $S(q)$ indicates the existence of ordered structure.

The first feature indicates that the phase (2a) is not an incommensurate phase. In order to understand the second feature we performed simulations with different Monte Carlo measurement times. If the time of measurement is not too long (e.g., 5×10^4 MC time steps at $T = 300K$) we observe (see Fig. 4a) that order in this structure changes

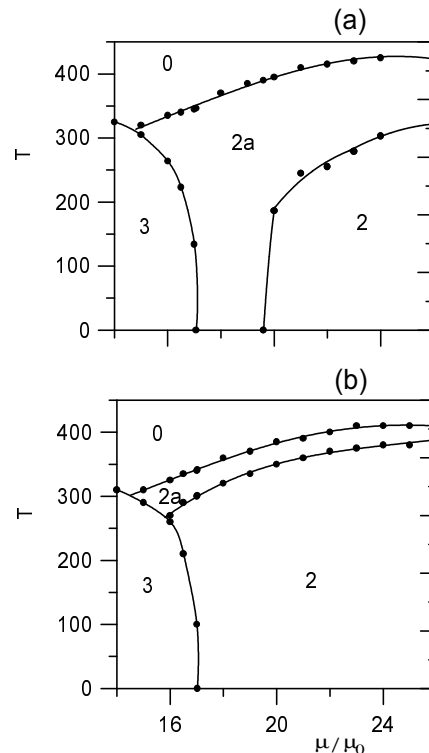


FIG. 3: Phase diagrams in the temperature / the chemical potential plane for (a) $Y_m = 72, L_y = 144$, (b) $Y_m = 36, L_y = 72$. Monte Carlo results are represented by circles.

spatially along y-direction. The disorder appears near domain walls but as one moves from the wall the chain structure emerges with increasing ordering. On the other hand we found that domain walls and the whole structure are moving along the y direction during simulation. This is a reason why the sublattice order parameters vanish if averaging time is long enough (see Fig. 4 where results of simulations with different averaging time are presented) but the structure factor remains finite.

A. Application to Li/W(112)

Linear chain structures (2×1) , (3×1) , and (4×1) were observed in the experiment of adsorption of lithium atoms on W(112) surface²³. Using MFA method, we have shown¹⁰ that lattice gas model, Eq. (1), describes such sequence of structures. Now we present results of Monte Carlo simulations. To avoid occurrence of phases with domain walls of (2a) type, we chose the range of indirect interaction equal to the linear size of the lattice along y direction, i.e., $Y_m = L_y$. Most simulations were performed on 20×72 lattice and sometimes the lattice of 40×72 sites was used. The range of dipole-dipole interaction was $R_m = 12a_y$. The ranges of these interactions used in previous MFA studies¹⁰ were both equal to $36a_y$. Therefore we also repeated the MFA calcula-

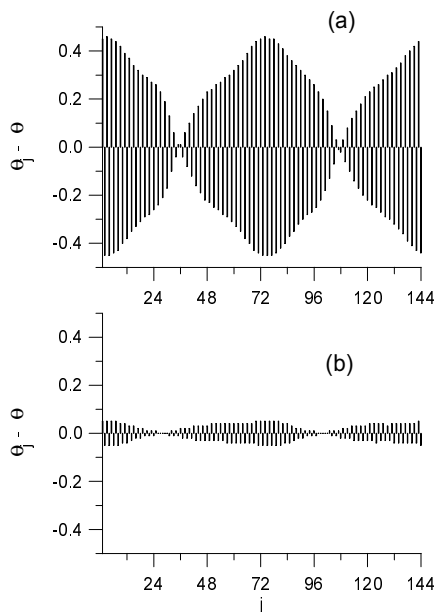


FIG. 4: The deviation of row coverage θ_j from the lattice coverage θ (denoted by bars) calculated at $T = 300K$, $\mu = 22\mu_0$, $Y_m = 72$, $L_y = 144$, and for averaging time (a) 5×10^4 (b) 10^6 MC steps per spin.

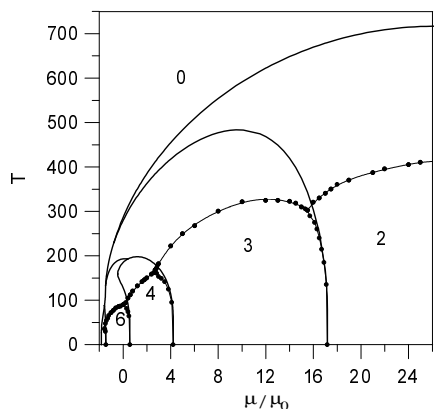


FIG. 5: Phase diagram in the temperature / the chemical potential plane for $Y_m = L_y = 72$. Mean-field results are denoted by thick lines and Monte Carlo results are represented by circles (a thin line serve as guide for an eye).

tions for present values of interaction ranges in order to compare the MFA results with Monte Carlo simulation results. As previously, MFA calculation were performed for all structures of $(p \times 1)$ type with p up to 12. In Fig. 5 we plot results of MFA and MC methods in the (T, μ) phase diagram. A low temperature part of the diagram does not depend on the method. However in the upper part of the diagram situation is quite different. Thermal fluctuations, not present in MFA, destroy ordered linear chains structures at temperatures much smaller than MFA critical temperature (the MFA critical

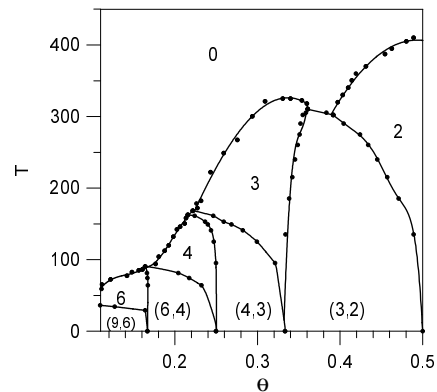


FIG. 6: Monte Carlo phase diagram in the temperature / coverage plane for $Y_m = L_y = 72$. Results of simulations are represented by circles.

temperature for the (2×1) phase can be even two times greater!). Moreover, MFA results do not allow to reach long periodic phases (4×1) and (6×1) directly from the disordered phase. On the other hand results of MC simulations show that all ordered phases can be reached from disordered phase in wide range of chemical potential. It is interesting to look at results of MC study presented in the (temperature - coverage) phase diagram (see Fig. 6). Ordered phases of $(p \times 1)$ are separated by mixed phases (p, p') which denotes mixture of $(p \times 1)$ phase and $(p' \times 1)$ phase. It is worth noting that ordered chain structures with period 6 and 9, present in the phase diagram, were not observed in experiments²³ which were performed at temperatures above 77K. We expect that these phases could be observed experimentally at temperatures below 77K.

Now, we are going to discuss the order of the phase transitions. The phase transitions between the ordered phases, e.g., $(2 \times 1) \rightarrow (3 \times 1)$, are of the first order because sublattice order parameters and structure factors change discontinuously at the transition points. The analysis of the phase transition from an ordered phase to the disordered phase is much more complicated. Checking temperature dependence of the structure factor and heat capacity (some results are shown in Fig. 7) we found that the transition to (9×1) and (6×1) phases is the first-order phase transition because of discontinuity of the structure factor. The transition to the (3×1) and (4×1) phases seems to be continuous transition. It is difficult to state the order of the phase transition from the disordered phase to the (2×1) phase. Although, the structure factor seems to be continuous function of temperature, the heat capacity is smeared near the transition temperature indicating the first-order phase transition. On the other hand, in the MFA calculation this phase transition is of the second order. One of possible explanation of this discrepancy is based on observation of additional, very weak maxima of the structure factor with the wave vector close to $q = (0, \pi/(a_y))$ and temperature in the

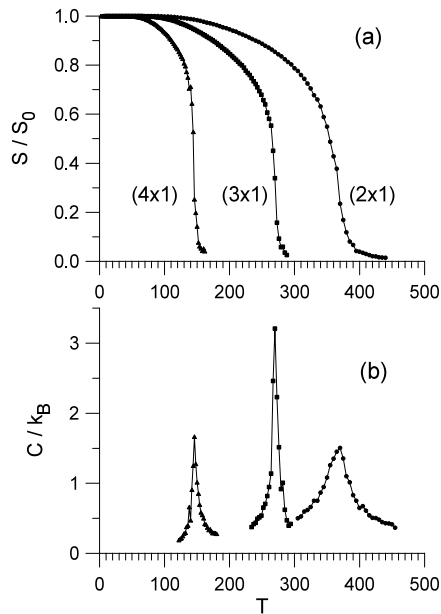


FIG. 7: Temperature dependence of (a) the structure factor (b) heat capacity in (4×1) , (3×1) , and (2×1) phases for $\mu/\mu_0 = 1.8, 6, \text{ and } 19$, respectively.

narrow range of the transition temperature. This can suggest that defected phases like the $2(a)$ phase are still present close to the transition temperature. In order to answer whether this problem is connected with the finite range of indirect interaction one should performed finite-size calculation with infinite range of the interaction. It can be done by employing a numerical method to accelerate the convergence of a Fourier series²⁴.

V. DISCUSSION AND CONCLUSIONS

Our Monte Carlo analysis revealed that truncation of the indirect interaction changes a phase diagram even if the interaction range is very large. New phases containing domain walls occur at high temperatures between the disordered phase and the $(p \times 1)$ phase. This problem complicates study of critical behaviour via finite-size scaling. One possible solution of such problem is accounting for infinite range of indirect interaction. It can be carried out by employing a numerical method to accelerate the convergence of a Fourier series²⁴ in the same way as in earlier paper¹¹. However, it would be time consum-

ing way to study the critical behaviour by Monte Carlo simulations. On the other hand it would be interesting to extend an analysis of defected phases (e.g., $(2a)$ phase) generated by truncation of indirect interaction. The structure factor of the $(2a)$ phase has maximum at the wavevector slightly shifted from the position which corresponds to maximum in the ordered (2×1) phase. Hence it might be important in analysis of LEED patterns.

Present MC calculations demonstrate that results of the mean field approximation are very bad especially at high temperatures. We have shown that MFA transition temperature from the disordered phase to the (2×1) phase is almost two times greater. Moreover, the high temperature part of the phase diagram has different topology than that obtained by MC simulations. However, it is interesting to note that both method give very similar results at low temperatures. Present MC calculations confirm earlier obtained results¹⁰ that at low coverages of lithium on the W(112) the long periodic structures (9×1) and (6×1) are stable at temperatures below 77K. It would be very interesting to determine experimentally the whole (T, Θ) phase diagram to check theoretical prediction. We are aware that present lattice gas model contains some phenomenological parameters, e.g., short range interaction E_b which has influence on the transition temperature. We think that the better way to estimate the model parameters is to perform the first-principles calculations of the interaction potentials in the Li/W(112) system.

Recently Yakovkin studied²⁵ chain structures adsorbed on Mo(112) and Re(1010) using lattice gas model in which the indirect interaction takes nonzero value only for one from all lattice distances. Performing MC simulations in canonical ensemble he was able to reconstruct the sequence of phases (4×1) and (2×1) as observed experimentally in Li/Mo(112). It is interesting whether such simple model could describe correctly the phases observed in adsorption of lithium on W(112).

We observed that Monte Carlo study of phase diagram in canonical ensemble is very difficult due to dependence of final MC results on initial lattice gas configuration. Although similar difficulty appears in grand canonical ensemble it is rather easy to find ground-state configurations and calculate free energies for different phases. However, it would be interesting to look for different algorithm than single spin flip in order to overcome the dependence MC results on initial configurations.

¹ A.G. Naumovets, Surf. Sci. 299/300 (1994) 706 and references cited therein.

² B.N.J. Persson, Surf. Sci. Rep. 15 (1992) 1.

³ A. Zangwill, Physics at Surfaces (Cambridge University Press, Cambridge, 1988).

⁴ O.M. Braun and V.K. Medvedev, Soviet Phys. Usp. 32 (1989) 328 and references cited therein.

⁵ L.A. Bolshov, A.P. Napartovich, A.G. Naumovets and A.G. Fedorus, Soviet Phys. Usp. 20 (1977) 432.

⁶ T.T. Tsong, Rep. Prog. Phys. 51 (1988) 759.

- ⁷ D. Kolthoff and H. Pfnür, Surf. Sci. 459 (2000) 265.
- ⁸ A. Fedorus, G. Godzik, V. Koval, A. Naumovets and H. Pfnür, Surf. Sci. 460 (2000) 229.
- ⁹ A. Fedorus, D. Kolthoff, V. Koval, I. Lyuksyutov, A.G. Naumovets and H. Pfnür, Phys. Rev. B 62 (2000) 2852.
- ¹⁰ F. Bagehorn, J. Lorenc and C. Oleksy, Surf. Sci. 349 (1996) 165 and references cited therein.
- ¹¹ C. Oleksy and J. Lorenc, Phys. Rev. B 54 (1996) 5955.
- ¹² D. Kolthoff and H. Pfnür, Surf. Sci. 457 (2000) 134.
- ¹³ G. Godzik, T. Block and H. Pfnür, Phys. Rev. B 67 (2003) 125424.
- ¹⁴ W. Selke, K. Binder and W. Kinzel, Surf. Sci. 125 (1983) 74.
- ¹⁵ K. Binder and D.P. Landau, Phys. Rev. B 21 (1980) 1941.
- ¹⁶ K. Binder, W. Kinzel and D.P. Landau, Surf. Sci. 117 (1982) 232.
- ¹⁷ K. Binder and D.P. Landau, Surf. Sci. 61 (1976) 577.
- ¹⁸ L.D. Roelofs and Donna L. Kriebel, J. Phys. C: Solid State Phys. 20 (1987) 2937.
- ¹⁹ I. Lyuksyutov, A.G. Naumovets and V. Pokrovsky, Two-Dimensional Crystals (Academic Press, Boston, MA, 1992).
- ²⁰ P. Bak and R. Bruinsma, Phys. Rev. Lett. 49 (1982) 249.
- ²¹ K. Sasaki, Surf. Sci. 318 (1994) L1230.
- ²² B. Gumhalter and W. Brenig, Surf. Sci. **336**, 326 (1995).
- ²³ V.K. Medvedev, A.G. Naumovets and T.P. Smereka, Surf. Sci. 34 (1973) 368.
- ²⁴ Cz. Oleksy, Comput. Phys. Commun. 96 (1996) 17.
- ²⁵ I.N. Yakovkin, Surf. Sci. 282 (1993) 195.